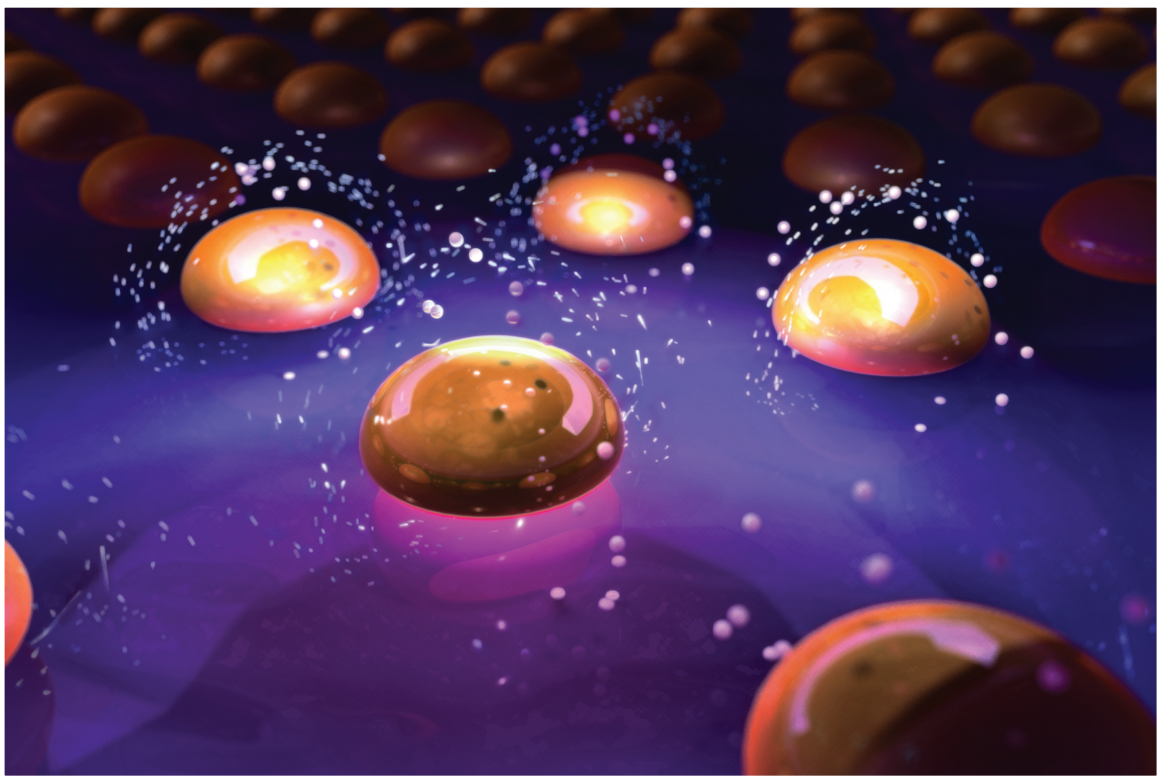


5 March 2012

Volume 100 Number 10

AIP | Applied Physics Letters



50th
Anniversary

apl.aip.org

Shifts in plasmon resonance due to charging of a nanodisk array in argon plasma

Michael Ian Lapsley, Anaram Shahravan, Qingzhen Hao, Bala Krishna Juluri, Stephen Giardinelli et al.

Citation: *Appl. Phys. Lett.* **100**, 101903 (2012); doi: 10.1063/1.3673327

View online: <http://dx.doi.org/10.1063/1.3673327>

View Table of Contents: <http://apl.aip.org/resource/1/APPLAB/v100/i10>

Published by the [American Institute of Physics](http://www.aip.org).

Related Articles

Quasi first-principles Monte Carlo modeling of energy dissipation by low-energy electron beams in multi-walled carbon nanotube materials

Appl. Phys. Lett. **100**, 093113 (2012)

Influence of a depletion layer on localized surface waves in doped semiconductor nanostructures

Appl. Phys. Lett. **100**, 091103 (2012)

A pancake-shaped nano-aggregate for focusing surface plasmons

J. Appl. Phys. **111**, 034308 (2012)

Plasmon assisted light propagation and Raman scattering hot-spot in end-to-end coupled silver nanowire pairs

Appl. Phys. Lett. **100**, 043108 (2012)

Energy-filtered phase retrieval using the transport of intensity equation

Appl. Phys. Lett. **99**, 221905 (2011)

Additional information on *Appl. Phys. Lett.*

Journal Homepage: <http://apl.aip.org/>

Journal Information: http://apl.aip.org/about/about_the_journal

Top downloads: http://apl.aip.org/features/most_downloaded

Information for Authors: <http://apl.aip.org/authors>

ADVERTISEMENT



LakeShore Model 8404 developed with **TOYO Corporation**
NEW AC/DC Hall Effect System Measure mobilities down to 0.001 cm²/V s

Shifts in plasmon resonance due to charging of a nanodisk array in argon plasma

Michael Ian Lapsley,¹ Anaram Shahravan,² Qingzhen Hao,^{1,3} Bala Krishna Juluri,¹ Stephen Giardinelli,¹ Mengqian Lu,¹ Yanhui Zhao,¹ I-Kao Chiang,¹ Themis Matsoukas,² and Tony Jun Huang^{1,a)}

¹Department of Engineering Science and Mechanics, The Pennsylvania State University, University Park, Pennsylvania 16802, USA

²Department of Chemical Engineering, The Pennsylvania State University, University Park, Pennsylvania 16802, USA

³Department of Physics, The Pennsylvania State University, University Park, Pennsylvania 16802, USA

(Received 15 November 2011; accepted 6 December 2011; published online 5 March 2012)

A method for generating charge-induced plasmonic shifts, using argon plasma to charge nanoparticle arrays, is presented. Particles develop a negative charge, due to enhanced collisions with high-temperature electrons, in low-temperature plasmas. The negative charge generated causes a blue shift in the localized surface plasmon resonance. The dynamics of the shift were recorded and discussed. This effect could be used as a real-time method for studying the dynamics for charging in plasma. © 2012 American Institute of Physics. [doi:10.1063/1.3673327]

Plasmonics deals with optically excited, oscillations of electrons at the interface between a metal and a dielectric,¹ and this phenomenon has driven the development of many optical devices.^{2–9} Surface plasmons excited in metal structures, confined at the nanoscale in three dimensions (i.e., nanoparticles, nanodisks, etc.), are known as localized surface plasmons. At certain wavelengths, maximum coupling from electromagnetic waves to localized surface plasmons can be achieved and these are known as the localized surface plasmon resonances (LSPRs) of the structure. LSPRs of metal nanostructures depend on properties such as the size,^{10,11} shape,^{12–14} metal material,¹⁵ surrounding dielectric material,^{16–22} and the charge of the metal.^{23–30} Active plasmonic devices can be realized by externally tuning the LSPR of nanostructures. Previously, chemical/electrochemical charging was used to actively tune the LSPR of arrays of both silver^{24,25,30} and gold^{23,26,27,29} nanostructures; however, this process is relatively slow. In this study, a rapid shift in the LSPR of an array of gold nanodisks was induced by surrounding the particles with a low-temperature argon plasma. This shift can be explained by the charging effect of the plasma.^{31–34} Charging by the plasma takes place in only seconds, where chemical/electrochemical charging can take several minutes²⁴ to hours.²⁷ This method allows real-time monitoring of the charging effect induced by low-pressure plasmas and could be utilized for photonics applications based on the LSPR shift.

In the experiment, the optical extinction spectrum of an array of gold nanodisks was measured while generating plasma. An array of gold nanodisks (diameters of 120 nm, thicknesses of 30 nm, and a periodicity of 300 nm) was fabricated on glass via electron-beam lithography.³⁵ A custom vacuum chamber was designed to include two flat, parallel windows to allow transmission of a probe light (Fig. 1(a)). The nanodisk array was placed inside the vacuum chamber

where it was attached to one of the flat windows. The probe light, ejected from the input optical fiber and collimated by a lens, traveled through the vacuum chamber and the sample. The output light was collected by the output lens/optical fiber and delivered to an optical spectrometer. A vacuum system was used to evacuate the chamber to a base pressure of 150 mTorr. Argon was introduced into the chamber using a mass flow controller. The argon gas was introduced at a flow rate of 6 SCCM and was ionized via an RF-driven, capacitively coupled, low-pressure discharge (30 W, 13.56 MHz) across two ring-shaped, aluminum electrodes.

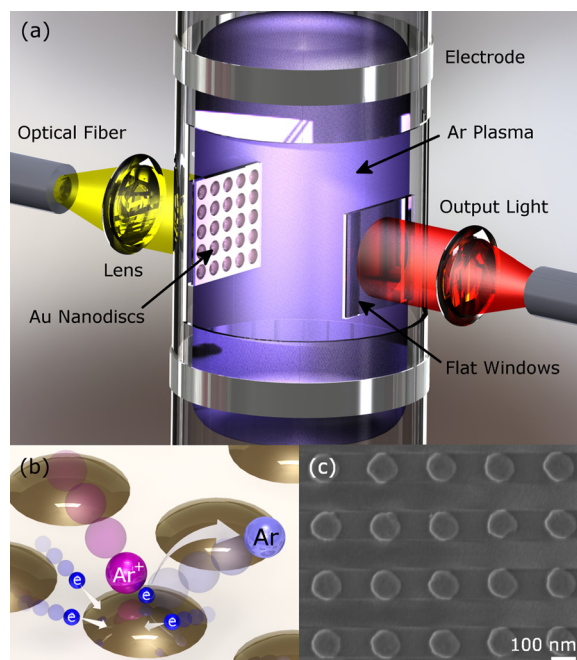


FIG. 1. (Color online) Experimental setup and device used in the experiment. (a) Schematic of the vacuum chamber, sample position, and optical setup. (b) Working mechanism for charging by plasma. (c) SEM image of the gold nanoparticles.

^{a)}Author to whom correspondence should be addressed. Electronic mail: junhuang@psu.edu.

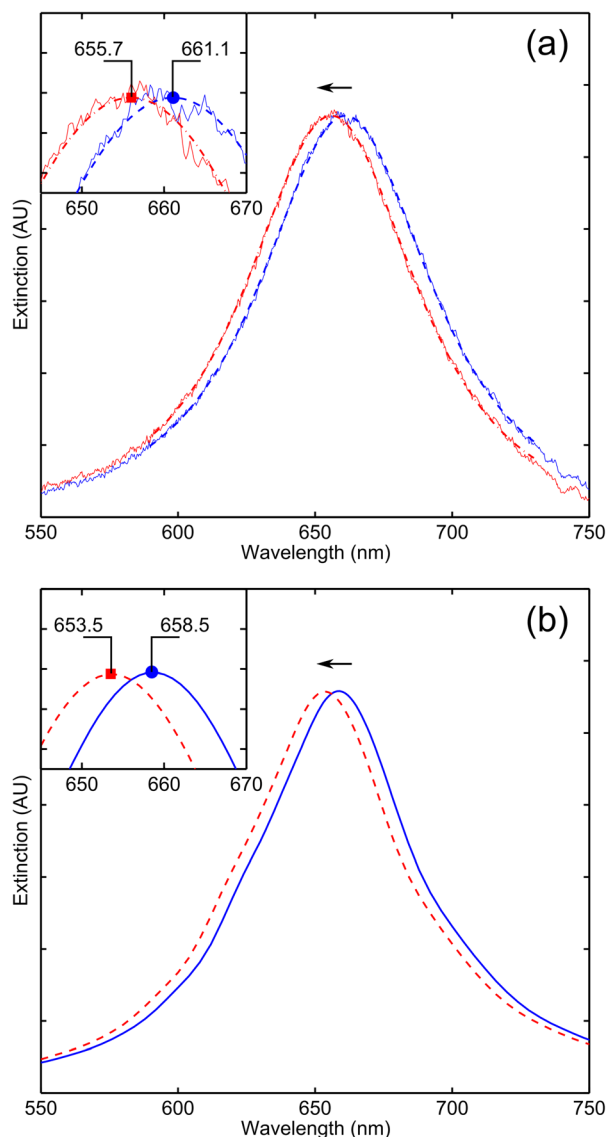


FIG. 2. (Color online) (a) Experimental extinction spectrum for gold nanodisk array. Raw data is shown as solid lines. The fitted curve for the initial position (dashed line) and the final position (dashed-dotted line) are shown as dashed lines. The insert displays a closer view of the peak positions. (b) The extinction spectra for the initial position (solid line) and the final position (dashed line) of the extinction spectrum simulated using DDA for the experimental conditions.

Argon plasma consists of a mixture of argon ions and free electrons, both of which are characterized by their own temperature. Electrons have a low mass and are quickly accelerated in the high-frequency electric field; the ions, whose mass is significantly higher, are not affected by the quickly alternating field. Consequently, the electrons acquire a high temperature while the ions are essentially at room temperature. The ions and the electrons collide with the gold nanodisks as shown schematically in Fig. 1(b). An electron collision injects a negative charge onto the particle, whereas an ion collision removes an electron. Since the electron temperature is higher than that of the ions, electron collisions happen more frequently, causing the particles to develop a negative net charge. Eventually, equilibrium is reached between the high probability of electron collisions and the repulsion of electrons due to the negative charge developed on the nanodisk.

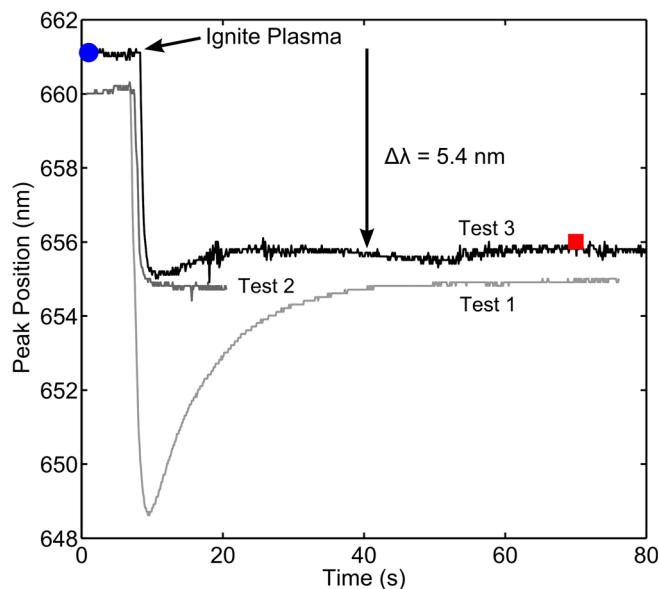


FIG. 3. (Color online) Dynamic response of the LSPR peak shift for three separate tests with a single nanodisk sample. The peak position of the fitted curve was recorded every 0.1 s. The blue circle and red square indicate the data points corresponding to the peak position of the initial and final curves plotted in Fig. 2(a), respectively.

Figure 2(a) displays the extinction spectrum for the sample before and after the plasma was ignited in the chamber. A curve was fitted to the raw data to determine the peak position. The fitted curve for each spectrum is shown as a dotted line over the raw data in Fig. 2(a), and its peak position was used to characterize shifts in the resonance spectrum. The initial peak position (λ_i) was 661.1 nm. When the plasma was generated, the peak position blue-shifted and settled at 655.7 nm (λ_f).

In order to study the dynamics and variability in the peak position during charging, a spectrum was recorded every 0.1 s during the experiment. A curve was fitted to each spectrum, and its peak position was plotted vs. time (Fig. 3, test 3). Data were collected for 10 s before igniting the plasma to record the initial variation, and the mean (μ) was 661.0835 nm with a standard deviation (σ) of 0.0734 nm. Immediately after igniting the plasma, the peak position blue-shifted. The initial shift happens in about 2 s with some overshoot lasting 10 s. With some optimization, the speed of this shift (~ 2 s) could be a major advantage of this technique as compared with electrochemical charging (>3 min).²⁴ After stabilization, the final position was analyzed ($\mu = 655.711$ nm, $\sigma = 0.1295$ nm). The plasma was active for another 1 min, while spectra were collected every 5 s ($\mu = 655.735$ nm, $\sigma = 0.0754$ nm). Subsequently, the plasma was removed, but no immediate red-shift was observed in the data. The peak position was monitored for about 5 more minutes yielding $\mu = 655.855$ nm and $\sigma = 0.1513$ nm. The slight increase in the μ and σ was due to mechanical vibrations altering the homogeneous broadening of the extinction spectrum. The plasma was reignited while spectra were again recorded every 0.1 s, but no blue-shift was observed. This entire data set was analyzed yielding $\mu = 656.453$ nm and $\sigma = 0.1325$ nm. The low standard deviation indicated that no significant change occurred throughout the second ignition of the plasma.

The plasma was extinguished, and the chamber was returned to atmospheric pressure. The sample was left in the test chamber at atmospheric pressure for 1 week, after which the LSPR red-shifted back to its initial position. The test was repeated three times with the same sample, and a similar pattern in the data was observed. In all three cases, the overall blue-shift was about 5 nm, and the discharge process lasted about 1 week. Essentially, the disks were charged by the initial exposure to the plasma and remained charged, as there was no path to electrical ground to allow discharging. Eventually, the electrons will discharge through the glass wall of the chamber, returning the particles to a neutral state. Tests 1, 2, and 3 all match closely ($\lambda_i \approx 660$ nm and $\lambda_f \approx 655$), with some differences in overshoot. The differences in each dataset are very interesting and need more exploration to fully verify the physical mechanism; however, a faster method for discharging the particles must be introduced.

Other phenomena, besides charging, have been shown to induce blue shifts in the LSPR spectrum which must be excluded as possible causes for the shift observed in this study. Reducing the size of particles via etching can cause a blue shift in the spectrum.¹¹ Etching is not a reversible process. In this study, the peak position eventually returned to its original state, indicating that etching did not occur. The deposition of dielectric material on the surface of the nanodisk array will cause a red shift and its removal would cause a blue shift.^{17–19} In this study, any material loosely adsorbed to the surface of the sample would be removed during the evacuation of the vacuum chamber, prior to data collection. Thus, the blue shift was not a result of etching or material removal.

The change in electron density, which is required to cause the LSPR shift observed in this study, was predicted by the following equation:³⁰

$$N_f = \frac{\lambda_i^2}{\lambda_f^2} N_i, \quad (1)$$

where N_i , 5.9×10^{28} electrons/m³, is the initial/uncharged free electron density for gold, and λ_i (661.1 nm) and λ_f (655.7 nm) are the initial and final peak positions of the extinction spectrum, respectively. The value of N_f for these conditions is 5.9976×10^{28} electrons/m³, yielding a percent change in charge density of 1.654%. Assuming the change in charge density calculated by Eq. (1), the disk geometry was simulated using the discrete dipole approximation (DDA) to predict the extinction spectrum.²⁶ Dielectric data for gold was predicted as in our previous work²⁶ and the surrounding dielectric was approximated as the root mean square of that of vacuum and glass. The results of this simulation are shown in Fig. 2(b), where the solid curve is the initial spectrum and the dotted curve is the final spectrum. The simulated curves were sharper and have peak positions at a slightly shorter wavelength. The peak shift in the simulations was 5 nm corresponding with the shift of 5.4 nm observed in the experiments. Despite the good results of this analysis, Eq. (1) is only valid for spherical particles with a radius much smaller than the wavelength; whereas, the particles used in this experiment are relatively large and disk-shaped. Also, others have observed that the increase in electron den-

sity calculated by Eq. (1) can be greatly exaggerated,²⁸ but the reason for this increase is currently unknown.

In conclusion, a method for shifting the LSPR of gold nanodisks was demonstrated. The nanodisks were charged by electron collisions in argon plasma. The nanodisks quickly charge in the plasma and remain charged for up to one week. Monitoring the LSPR allows a real-time method for analyzing the charging effect induced by plasma. The process was repeatable and its dynamics were faster than other charge-based shifting methods. Optimization of the charging and discharging of the nanodisks could allow the rapid switching response to be utilized as an optical device.

¹S. Maier, *Plasmonics: Fundamentals and Applications* (Springer, Berlin, 2007).

²L. Feng, A. Mizrahi, S. Zamek, Z. Liu, V. Lomakin, and Y. Fainman, *ACS Nano* **5**, 5100 (2011).

³D. E. Gomez, K. C. Vernon, P. Mulvaney, and T. J. Davis, *Appl. Phys. Lett.* **96**, 073108 (2010).

⁴D. E. Gomez, K. C. Vernon, P. Mulvaney, and T. J. Davis, *Nano Lett.* **10**, 274 (2010).

⁵D. Lu, J. Kan, E. E. Fullerton, and Z. Liu, *Appl. Phys. Lett.* **98**, 243114 (2011).

⁶C. Ma and Z. Liu, *J. Nanophotonics* **5**, 051604 (2011).

⁷W. Srituravanich, L. Pan, Y. Wang, C. Sun, D. B. Bogy, and X. Zhang, *Nat. Nanotechnol.* **3**, 733 (2008).

⁸Y. Wang, W. Srituravanich, C. Sun, and X. Zhang, *Nano Lett.* **8**, 3041 (2008).

⁹Y. Zhao, S.-C. S. Lin, A. A. Nawaz, B. Kiraly, Q. Hao, Y. Liu, and T. J. Huang, *Opt. Express* **18**, 23458 (2010).

¹⁰M. K. Kinnan and G. Chumanov, *J. Phys. Chem. C* **114**, 7496 (2010).

¹¹Y. B. Zheng, L. Jensen, W. Yan, T. R. Walker, B. K. Juluri, L. Jensen, and T. J. Huang, *J. Phys. Chem. C* **113**, 7019 (2009).

¹²C. L. Nehl and J. H. Hafner, *J. Mater. Chem.* **18**, 2415 (2008).

¹³C. Orendorff, T. Sau, and C. Murphy, *Small* **2**, 636 (2006).

¹⁴K. C. Vernon, A. M. Funston, C. Novo, D. E. Gomez, P. Mulvaney, and T. J. Davis, *Nano Lett.* **10**, 2080 (2010).

¹⁵J.-H. Kim, W. W. Bryan, and T. R. Lee, *Langmuir* **24**, 11147 (2008).

¹⁶Q. Hao, Y. Zhao, B. K. Juluri, B. Kiraly, J. Liou, I. C. Khoo, and T. J. Huang, *J. Appl. Phys.* **109**, 084340 (2011).

¹⁷J. Heckel, F. Farhan, and G. Chumanov, *Colloid Polym. Sci.* **286**, 1545 (2008).

¹⁸M. K. Kinnan, S. Kachan, C. K. Simmons, and G. Chumanov, *J. Phys. Chem. C* **113**, 7079 (2009).

¹⁹E. M. Larsson, J. Alegret, M. Käll, and D. S. Sutherland, *Nano Lett.* **7**, 1256 (2007).

²⁰Y. J. Liu, Q. Hao, J. S. T. Smalley, J. Liou, I. C. Khoo, and T. J. Huang, *Appl. Phys. Lett.* **97**, 091101 (2010).

²¹C. Sun, K.-H. Su, J. Valentine, Y. T. Rosa-Bauza, J. A. Ellman, O. Elboudwarej, B. Mukherjee, C. S. Craik, M. A. Shuman, F. F. Chen *et al.*, *ACS Nano* **4**, 978 (2010).

²²Y. B. Zheng, Y.-W. Yang, L. Jensen, L. Fang, B. K. Juluri, A. H. Flood, P. S. Weiss, J. F. Stoddart, and T. J. Huang, *Nano Lett.* **9**, 819 (2009).

²³T. Baum, D. Bethell, M. Brust, and D. J. Schiffrin, *Langmuir* **15**, 866 (1999).

²⁴R. Chapman and P. Mulvaney, *Chem. Phys. Lett.* **349**, 358 (2001).

²⁵J. K. Daniels and G. Chumanov, *J. Electroanal. Chem.* **575**, 203 (2005).

²⁶B. K. Juluri, Y. B. Zheng, D. Ahmed, L. Jensen, and T. J. Huang, *J. Phys. Chem. C* **112**, 7309 (2008).

²⁷P. Mulvaney, J. Pérez-Juste, M. Giersig, L. Liz-Marzán, and C. Pecharromán, *Plasmonics* **1**, 61 (2006).

²⁸A. C. Templeton, J. J. Pietron, R. W. Murray, and P. Mulvaney, *J. Phys. Chem. A* **104**, 564 (2000).

²⁹A. Toyota, N. Nakashima, and T. Sagara, *J. Electroanal. Chem.* **565**, 335 (2004).

³⁰T. Ung, M. Giersig, D. Dunstan, and P. Mulvaney, *Langmuir* **13**, 1773 (1997).

³¹T. Matsoukas, *J. Aerosol Sci.* **25**, 599 (1994).

³²T. Matsoukas and M. Russell, *J. Appl. Phys.* **77**, 4285 (1995).

³³T. Matsoukas and M. Russell, *Phys. Rev. E* **55**, 991 (1997).

³⁴A. Shahravan, C. Lucas, and T. Matsoukas, *J. Appl. Phys.* **108**, 083303 (2010).

³⁵Q. Hao, Y. Zeng, X. Wang, Y. Zhao, B. Wang, I.-K. Chiang, D. H. Werner, V. Crespi, and T. J. Huang, *Appl. Phys. Lett.* **97**, 193101 (2010).